High magnetic field x-ray diffraction study of the α phase of solid oxygen: Absence of giant magnetostriction

Yasuhiro H. Matsuda ●,* Ayumi Shimizu, Akihiko Ikeda, Toshihiro Nomura, and Takeshi Yajima
The Institute for Solid State Physics, The University of Tokyo,5-1-5 Kashiwa, Chiba 277-8581, Japan

Toshiya Inami
Synchrotron Radiation Research Center, National Institutes for Quantum and Radiological Science and Technology, Sayo, Hyogo 679-5148, Japan

Kohki Takahashi ●
Institute for Materials Research, Tohoku University, 2-1-1 Katahira, Aobaku, Sendai 980-8577, Japan

Tatsuo C. Kobayashi
Department of Physics, Okayama University, Okayama 700-8530, Japan

High magnetic field x-ray diffraction experiments of solid oxygen have been performed at 10 K using DC magnetic fields of up to 5 T as well as pulsed magnetic fields of up to 25 T. The α phase of oxygen exhibits no magnetostriction greater than $\Delta d/d = 10^{-4}$ at 5 T, where d and Δd denote a lattice plane spacing and its magnetic field variation, respectively. The $\Delta d/d$ at higher fields of up to 25 T is found to be smaller than 2×10^{-3}. These results contradict the previously reported giant magnetostriction in the α phase where the volume magnetostriction $\Delta V/V$ reaches 10^{-2} at 7.5 T [K. Katsumata *et al.*, J. Phys.: Condens. Matter **17**, L235 (2005)].

I. INTRODUCTION

Solid oxygen is a unique magnetic material in terms of competition between the van der Waals cohesive energy and the magnetic intermolecular potential. The spin degree of freedom strongly couples to the lattice degree of freedom because the exchange interaction between spins of molecules depends on the steric configuration of molecules [1]. As results of the strong spin-lattice coupling, several structural phase transitions occur by changing an external environmental parameter such as temperature, pressure, and magnetic field [2,3]. For instance, with decreasing temperature, the liquid-γ, γ-β, and β-α transitions occur at 54.4, 43.8, and 23.9 K, respectively, developing the antiferromagnetic correlation between $S = 1$ spins of molecules (S is the quantum spin number). The high magnetic field θ phase has recently been discovered in 100 T field range [4–6] and the novel crystal structure appears due to rearrangement of the molecular configuration as clear experimental evidence of the strong spin-lattice coupling. Although one of the promising crystal structures is cubic ($Pa\bar{3}$) [7], the actual crystal structure of the θ phase has not been experimentally confirmed yet because of the required ultrahigh magnetic field.

The direct observation of magnetic field effect on the crystal lattice of solid oxygen was investigated using x-ray diffraction (XRD) [8], and the magnetovolume striction $\Delta V/V$ was reported to be as large as 1% at 7.5 T in the α phase. The changes in the a and b lattice constants at 7.5 T are $\Delta a/a \sim 5.2 \times 10^{-3}$ and $\Delta b/b \sim 7.6 \times 10^{-3}$, respectively, and their field dependences seem to be linear shape. The change in the c axis and that in the angle between the a and c axes were reported to be rather small compared to those along the a and b axes. The observed striction, which is much larger than that in ferromagnetic metals such as Fe ($\Delta V/V \sim 0.004\%$ at 8 T), was termed as giant magnetovolume effect [8].

In the present study, we have performed XRD experiments in high magnetic fields using a DC magnet up to 5 T as well as a pulsed magnet up to 25 T, aiming to investigate the giant magnetostriction of the α phase of solid oxygen. In Sec. II, the details of the experimental setups are explained. The experimental results are shown in Sec. III. Our results did not reproduce the previously reported giant magnetovolume effect. The obtained results are discussed in terms of technical as well as physical points of view in Sec. IV. The conclusions of this work are given in Sec. V.

II. EXPERIMENT

The high-field XRD experiments have been performed at the Institute for Materials Research of Tohoku University with a DC magnet up to 5 T, and at BL22XU in SPring-8 up to 25 T using a pulsed magnet. Pure oxygen gas (purity > 99.99995%) was liquified by cooling into a sample cell designed for each experiment. The setups for the XRD experiments around the sample space are shown in Figs. 1(a)
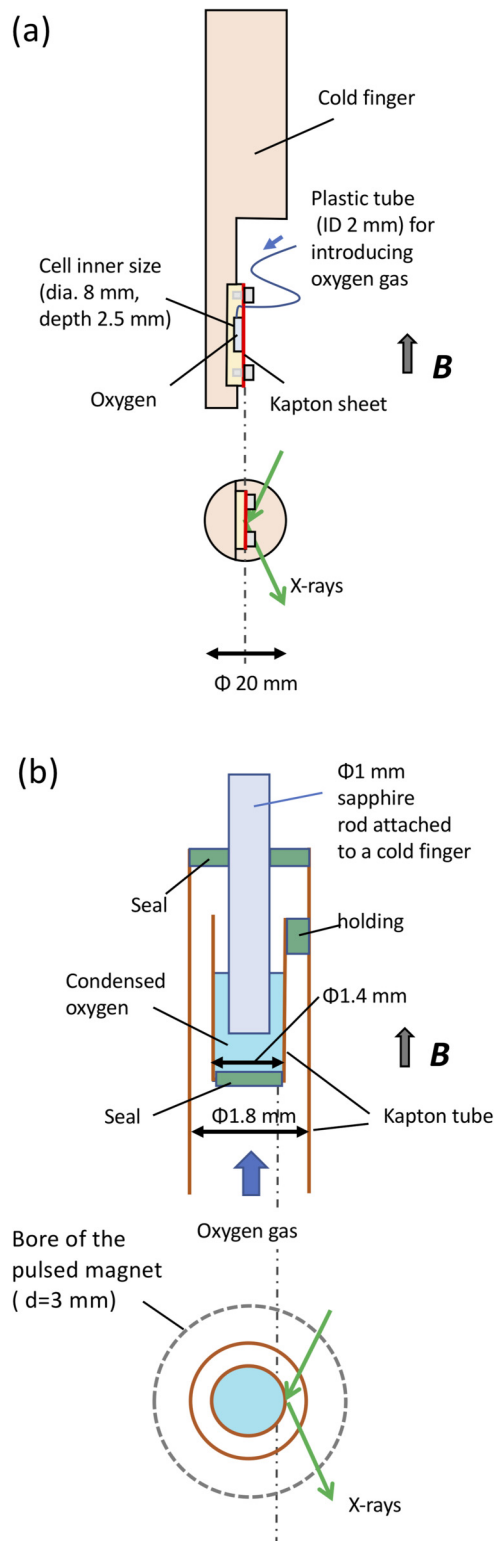
*ymatsuda@issp.u-tokyo.ac.jp

FIG. 1. (a) Experimental setup around the sample for the 5 T DC magnetic field [9]. (b) Experimental setup around the sample for the 25 T pulsed magnetic field [11].

and 1(b). Magnetic fields were applied perpendicular to the direction of the incident and diffracted x rays in both measurements. A split-pair magnet with windows for XRD experiments was used for each experiment [9–11].
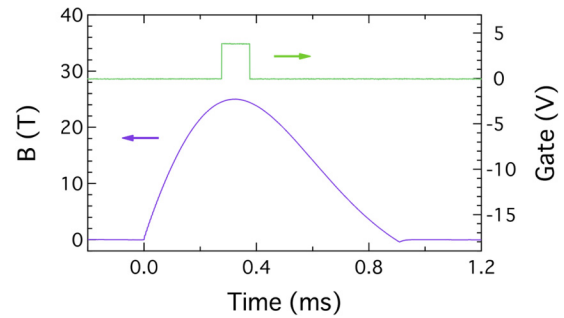

FIG. 2. The waveform of the pulsed magnetic field and the gate pulse for the x-ray detector.

For the 5 T DC-magnet experiment, a Cu $K\alpha$ (1.54 Å) characteristic emission line was used as the x-ray source. A helium-gas-closed-cycle refrigerator (so-called GM cryocooler) was used for cooling the 5 T superconducting magnet as well as the sample [9]. A scintillation counter was used as the x-ray detector. The measurement temperature was controlled to be 10 K.

In the 25 T pulse-magnet experiments, the photon energy (wavelength) of the synchrotron x-ray used is 15 keV (0.8266 Å). The diffraction data were recorded with a PILATUS 100 K detector system [12]. Another GM cryocooler was used for cooling the sample as well as the pulsed magnet [11]. The time interval of the successive pulsed magnetic field measurements is 10–20 min, which is necessary for cooling the magnet after heating due to the discharge for field generation. The pulsed magnetic field XRD measurements have been done in time domain [10,11,13]. The gate pulse that initiates recording the diffraction profile in the PILATUS 100 K detector has a 100 μs duration time and was controlled to be located at the peak of the pulsed magnetic field waveform as shown in Fig. 2. The variation of the magnetic field $\Delta B/B$ during the measurement time (100 μs) is around 2%.

III. RESULTS

A. XRD in the 5 T DC magnetic field

Figure 3(a) shows XRD profiles at several diffraction angle (2θ) regions in 0 and 5 T. It is found that the 001, −111, and −201 Bragg peaks shift to a small-angle region by applying 5 T, while 020, −312, and 021 peaks show no clear peak shift by magnetic field.

Because the diffractometer equipped with a DC magnet can be mechanically affected by the magnetic field [9], we measured the XRD of Cu as the reference data in magnetic fields. We used the surface of the Cu plate of the sample cell shown in Fig. 1. The vertical position of the sample holder was moved upward by 6 mm so that the x ray shines the surface of the Cu plate whose position is identical to the sample position before the 6 mm vertical movement. The observed diffraction profiles are shown in Fig. 4. The double peak structure corresponds to the energy splitting of the incident x rays $K\alpha_1$ (1.5405 Å) and $K\alpha_2$ (1.5443 Å). Similar splitting of the diffraction peaks is not seen in the results of solid oxygen as shown in Fig. 3(a) because their diffraction peaks are broad. In Fig. 4, it is found that the 111 and 020 diffraction peaks of the Cu slightly shift to the smaller 2θ region by applying 5 T.
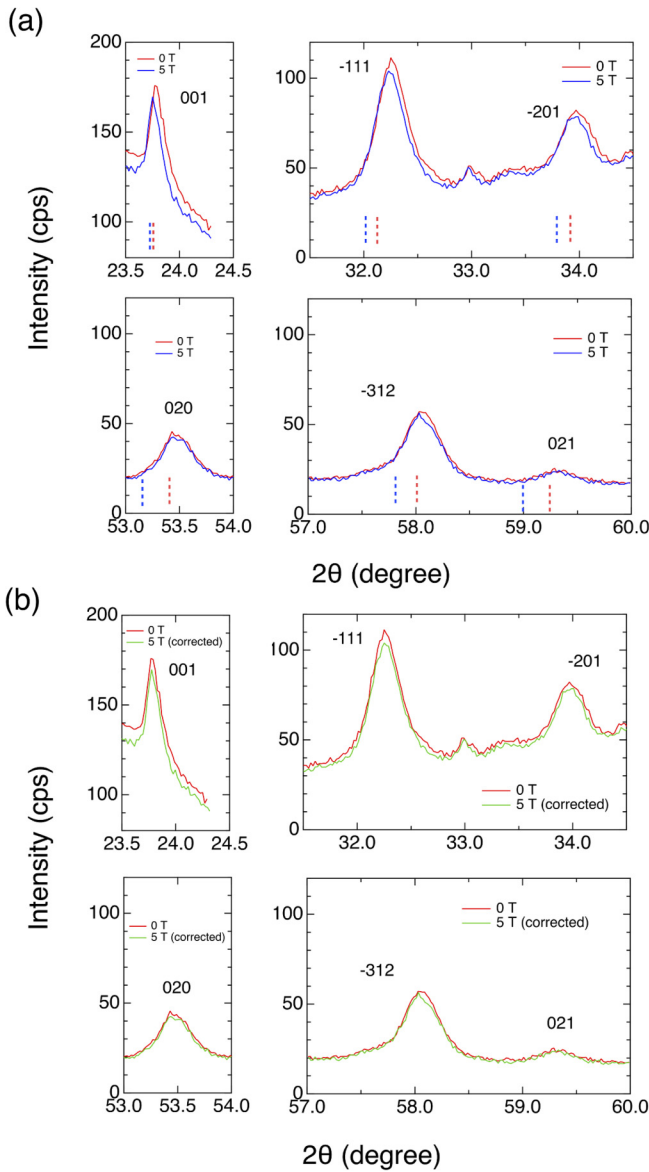
FIG. 3. (a) XRD profiles of the α phase of solid oxygen at 0 and 5 T. The measurement temperature is 10 K. The used x ray is the Cu $K\alpha$ line (1.54 Å). The red and blue dashed lines denote the expected positions of the diffraction peaks using the reported lattice parameters at 0 and 5 T in the previous work [8]. (b) XRD profiles of the α phase of solid oxygen at 0 and 5 T after the correction of the experimental error in 2θ. The measurement temperature is 10 K. The details of the correction are described in Sec. IV.

We use this result to calibrate the recorded diffraction angle 2θ and the corrected XRD profiles are shown in Fig. 3(b). The details of the correction are described in Sec. IV.

B. XRD in pulsed magnetic fields of up to 25 T

The measured XRD profiles in pulsed magnetic fields at 10 and 25 T are shown in Fig. 5 along with the zero-field profile. The XRD at 0 T is measured with an exposure time of 10 ms. The profiles at 10 and 25 T are obtained by averages of six times and five times repetition of the measurements, respectively. The 001 and -111 peaks are clearly observed,
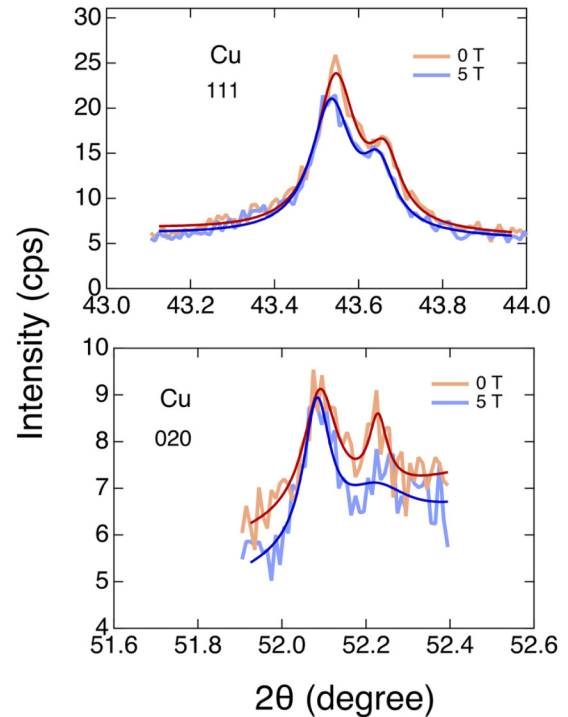

FIG. 4. XRD profiles of Cu from the surface of the sample holder at 0 and 5 T. The measurement temperature is 10 K. The used x ray is the Cu $K\alpha$ line (1.54 Å). The thick curves are data obtained by smoothing the original data shown with washy colors.

while the -201 peak is seen as a shoulder of the -111 peak. The obtained XRD profiles at different magnetic fields seem to be identical at first glance.

IV. DISCUSSIONS

We first discuss the obtained XRD profiles at 5 T. In Fig. 3(a), the red and blue dashed lines are the expected diffraction peak positions at 0 and 5 T, respectively, using the lattice parameters reported in the previous work [8]. The peak positions at 0 T are observed at a slightly higher angle in
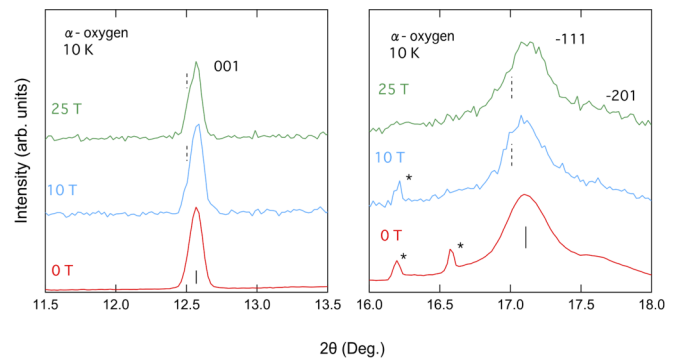

FIG. 5. 001, -111, and -201 XRD profiles in the α phase at 0, 10, and 25 T. Diffraction peaks with * probably come from impurities adopted on the Kapton tube around the condensed oxygen. The thin vertical line denotes the peak position at 0 T and the thin dashed lines denote the peak position deduced using the magnetic field effect on the lattice parameters at 7.5 T reported in the previous work [8].
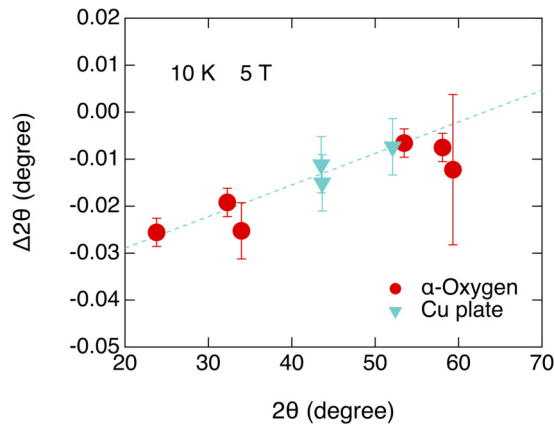
FIG. 6. The observed peak shifts in 2θ at 5 T in the α phase of solid oxygen and Cu of the surface of the sample holder.

FIG. 7. The relative changes of the diffraction plane spacing at 5 T are shown at different reciprocal vectors.

the present work. According to the previous work, the lattice constants of the *a*, *b*, and *c* axes increase with magnetic fields, and the XRD peaks should shift to a lower angle as indicated by the blue dashed lines.

The magnetic field effect on the 001, −111, and −201 peaks we observed seem to be in agreement with the results of the previous study. However, it is not for 020, −312, and 021 peaks. Although these peaks should show a larger field-induced shift than the lower angle diffraction peaks such as 001, −111, and −201, the actually observed field-induced shift is smaller as shown in Fig. 3(a). This finding strongly suggests that there must be an experimental error caused by magnetic field effects on the diffractometer.

Therefore, the observed magnetic field effect on the XRD of solid oxygen in the present work should be corrected by some reference data. We believe that the surface of the sample holder made of Cu is a good reference sample. Almost no magnetic field effect on the crystal lattice of Cu is expected to be observed at 5 T. Hence, the XRD peak must show no change in the position by the magnetic field. In other words, the XRD profiles of oxygen shown in Fig. 3(a) have to be corrected so that the XRD of Cu keeps the diffraction angle independent of magnetic fields.

In Fig. 6, the changes in 2θ by applying 5 T are plotted for different diffraction peaks. The error bar of the peak position of the 021 peak at around 59.3° is relatively large because of its small intensity. The dashed line represents the linear background obtained from the least-square fit for the 111 and 020 peaks of Cu. We use this background for calibrating the angle positions of the diffraction peaks. The $\Delta 2\theta$ is subtracted from the measured 2θ for the measurement of oxygen at 5 T for each angle.

The XRD profiles of the α phase of solid oxygen after the calibration are shown in Fig. 3(b). The diffraction peaks show no clear peak shift by applying magnetic fields. By contrast that the calibration is expected to be accurately applied for the 020 and −312 peaks, it might be less accurate in the lower-angle peaks such as 001, −111, and −201.

The relative change in the layer spacing (*d*) for each diffraction plane by applying a magnetic field of 5 T is plotted in Fig. 7 as a function of the absolute value of the reciprocal lattice vector $q = 2\pi/d$. It is found that no significant change
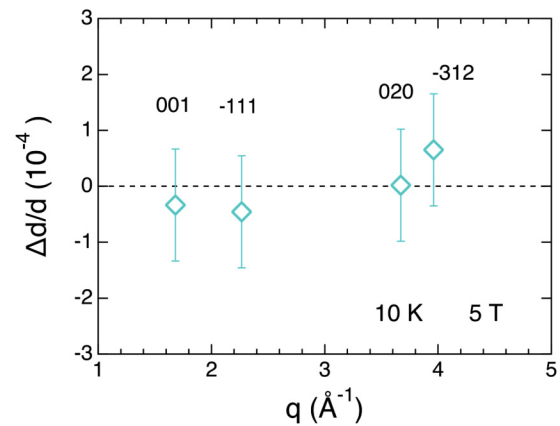
in the spacing of the diffraction layer *d* is induced by applying 5 T. The linear magnetostriction is smaller than 10^{-4} at 5 T, which contradicts the results in the previous work [8] in which 10^{-3} or larger value is reported at 5 T.

The magnetic field effects on the XRD at 10 and 25 T are also smaller than that expected from the reported magnetostriction. According to the previous work [8], *d* of the (001) diffraction plane and that of the (−111) plane are expected to increase with magnetic field, and the relative increases of $\Delta d/d$ at 7.5 T are evaluated to be 5.2×10^{-3} and 5.9×10^{-3}, respectively. The diffraction peaks are expected to shift to lower 2θ positions and they are indicated with the thin dashed lines in Fig. 5. However, the diffraction peaks observed at 10 and 25 T are located at the same position as that at 0 T within our measurement resolution. It is worth noting that the experimental error caused by applied magnetic fields similar to the 5 T DC-field measurements is not expected to exist in the pulsed magnetic field measurements. This is because the volume of the magnet is small [10,11,14] and thus the leak-field effect on the measurement apparatus is almost negligible. Although mechanical vibration due to the magnetic field pulse can cause a disturbance of the sample position, the effect is not significant when the pulse duration is shorter than around 1 ms. The mechanical movement of the sample holder generally takes a longer time and does not disturb the detection of the diffracted x rays [10,11,14].

The $\Delta d/d$ for the (001) and (−111) planes are plotted as a function of the magnetic field in Fig. 8. The magnetic field dependences of $\Delta d/d$ for the (001) and (−111) planes obtained from the crystal-lattice parameters previously reported are also shown. The magnetic field effect observed in the present study is not greater than $\Delta d/d = 10^{-4}$ at 5 T, and the upper limit of $\Delta d/d$ at 25 T is 2×10^{-3}, which is much smaller than the reported giant magnetostriction.

Here we simply evaluate the energy balance between the magnetic energy ($-MH$, where *M* and *H* here denote the magnetization and the applied magnetic field, respectively) and the elastic energy. The magnetization of the α oxygen is about 5.6 emu/g [15] at 8 T and the magnetic energy is deduced to be −1.41 J/mol. As for the elastic energy, we can roughly estimate it using the bulk modulus 2.97 GPa [16] and the volume magnetostriction $\Delta V/V$. If $\Delta V/V = 10^{-2}$, the
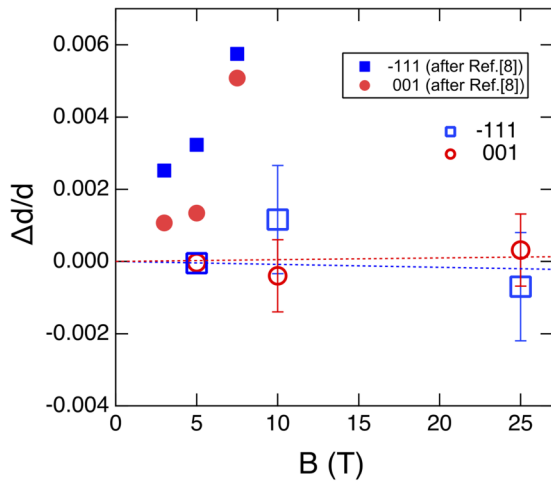
FIG. 8. The relative change in the spacing ($\Delta d/d$) of the (-111) diffraction plane is plotted as a function of magnetic field with open squares. The $\Delta d/d$ of the (001) diffraction plane is plotted as a function of magnetic field with open circles. The dotted red and blue lines are results of the least-square linear fitting to the experimental results of the 001 and -111 diffractions, respectively. Calculated $\Delta d/d$ at 3, 5, and 7.5 T for -111 and 001 diffractions using the reported magnetic field dependence of the crystal-lattice parameters [8] are plotted with closed squares and closed circles, respectively.

elastic energy is deduced to be 6.17×10^2 J/mol, which is more than two orders of magnitude larger than the magnetic energy.

By contrast, the magnetic energy of liquid oxygen is evaluated to be -5.85 J/mol at 8 T [17], while the elastic energy is deduced to be 6.12 J/mol [18]. The agreement in order between the elastic energy and the magnetic energy is understandable, although the energy relaxed due to the magnetostriction mechanism must be smaller than the absolute value of the magnetic energy.

In the previous report [8], the exchange striction mechanism is raised as the origin of the giant magnetostriction. The exchange striction is the effect that deformation of the crystal lattice takes place so that a resultant change in the exchange interaction increases the magnetization. Hence, part of the magnetic energy can be saved by an exchange striction mechanism, and it should be in balance with an increase of the elastic energy.

If we assume $\Delta V/V \sim 10^{-5}$ at 8 T for α oxygen, the elastic energy becomes comparable to the absolute value of the magnetic energy. In this case, the linear magnetostriction expected is as large as $\sim 2 \times 10^{-6}$ at 5 T and $\sim 10^{-5}$ at 25 T, which is smaller than the resolution limit for detecting the change in the lattice with XRD in the present work. Moreover, the linear magnetostriction as large as 10^{-6} T^{-1} has recently been observed by means of the fiber Bragg grating (FBG) strain gauge [19,20] in α oxygen at 4 K up to 30 T [21]. This finding supports the results of our XRD experiments. The giant volume magnetostriction $\Delta V/V = 10^{-2}$ at 7.5 T reported in the previous study [8] is more than two orders of magnitude larger than our results of XRD and that of magnetostriction. It may also be worth noting that modes of the electron spin resonance up to 50 T of α oxygen is

well explained in terms of the molecular field theory with the parameters independent of magnetic field [22,23], which indicates that no significant exchange striction occurs.

The reason for the contradiction between our results and the previous study is not very clear. Although the measurement temperature (1.5 K) was lower in the previous study, the discrepancy of the observed magnetostriction is likely to be too large because no drastic change in the material properties has been seen in α oxygen between 10 and 1.5 K. One of the possible causes for the contradiction is that there had been some mechanical influence on the experimental configuration by applying DC magnetic fields in the previous work as we had observed in the 5 T DC-field measurement. Small mechanical movements of measurement apparatuses can cause a change in the observed XRD peak positions.

Here we evaluate the possible technical error in measuring 2θ. It is assumed that a sample holder becomes slightly bent when a magnetic field is applied and the sample moves from the center position. The movement is approximated to be in the diffraction plane. As shown in Fig. 9(a), the position of the detector is changed from position A to position A′ and the change in 2θ is defined as $\Delta 2\theta = 2\theta' - 2\theta$. The coordinates of A and A′ can be defined as A $= (L\cos 2\theta, L\sin 2\theta)$ and
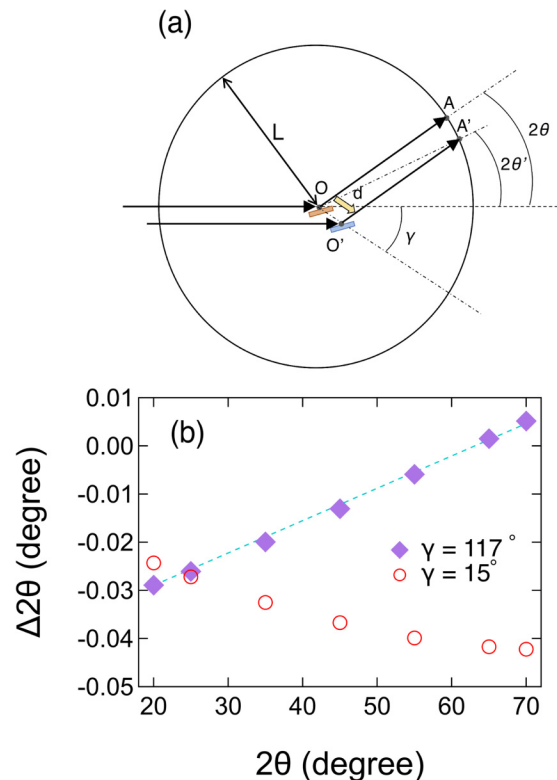

FIG. 9. (a) The schematic view of effects of sample position displacement from the center of a diffractometer. The displacement vector $\boldsymbol{d}$ is represented by the thick arrow. It is assumed that the detected diffraction angle 2θ is changed to $2\theta'$ by the sample displacement when a magnetic field is applied. (b) The changes in the diffraction angle $\Delta 2\theta = 2\theta' - 2\theta$ are plotted as a function of 2θ with different angles γ. A condition $L = 500$ mm and $d = 0.37$ mm is used. The dashed line represents the calibration line used for the correction of the diffraction angle shown in Fig. 6.

A$' = (x, y)$. O is the origin of the coordinate system and $\boldsymbol{d} = \overrightarrow{OO'}$. The $2\theta'$ is numerically obtained using the following equations.

$$\frac{x - d\cos\gamma}{L\cos 2\theta} = \frac{y + d\sin\gamma}{L\sin 2\theta}, \tag{1}$$

$$x^2 + y^2 = L^2, \tag{2}$$

$$2\theta' = \tan^{-1}(y/x). \tag{3}$$

The angle γ represents the direction of the sample displacement vector $\boldsymbol{d}$. If the amount of the displacement $|\boldsymbol{d}| = d$ is smaller than the x-ray beam spot, the configuration shown in Fig. 9(a) is not far from the real situation.

Calculated $\Delta 2\theta$ are plotted as a function of 2θ in Fig. 9(b). $L = 500$ mm is used and it corresponds to the actual size of the diffractometer used in the present work for the 5 T measurement. It is found that when $\gamma = 117°$, $d = 0.37$ mm provides very good agreement with the $\Delta 2\theta$ experimentally observed (Fig. 6). The 2θ dependence of $\Delta 2\theta$ becomes qualitatively different by a change in γ from 117° to 15°. The $\Delta 2\theta$ becomes small if $\boldsymbol{d}$ is parallel to the diffracted x ray; $\Delta 2\theta \sim 0$ at $2\theta = 63° = 180° - 117°$ for $\gamma = 117°$.

It is worth noting that this phenomenon due to the mechanical position change has nothing to do with the XRD index. Because the result, similar to that for $\gamma = 15°$, can also be obtained by physically meaningful reasoning (i.e., crystal deformation), one should be careful when collecting and analyzing the XRD data obtained in DC magnetic fields. Since the leak field of a superconducting magnet is relatively strong, a structural object holding a sample can be influenced by a magnetic field applied even if it is made from a nonmagnetic metal. This is because the holder is attached to the diffractometer and the diffractometer has parts made from a magnetic metal, more or less. Moreover, a nonmagnetic metal may become magnetic at low temperatures due to impurities.

V. CONCLUSIONS

The high-field XRD experiments on α oxygen at 10 K has revealed that the linear magnetostriction $\Delta d/d$ is smaller than 10^{-4} T^{-1} in magnetic fields of up to 25 T. Simple order estimation of the elastic energy compared to the magnetic energy indicates that the previous report on the magnetostriction of liquid oxygen $\Delta V/V = 2 \times 10^{-4}$ at 8 T is reasonable, while the reported magnetostriction [8] of α oxygen $\Delta V/V = 10^{-2}$ at 7.5 T is more than two orders of magnitude larger than the expected value. A more detailed theoretical analysis would be necessary for quantitative discussions.

The absence of the giant magnetostriction in α oxygen may also be in agreement with the experimental fact that the magnetic field induced α-θ transition is first order [4–6]. The deformation of the crystal lattice in a magnetic field is not significant below the critical magnetic field around 100 T. It is likely that a drastic symmetry change in the crystal lattice takes place discontinuously at the phase transition.

[1] B. Bussery and P. E. S. Wormer, J. Chem. Phys. **99**, 1230 (1993).

[2] Yu. A. Freiman and H. J. Jodl, Phys. Rep. **401**, 1 (2004).

[3] Yu. A. Freiman, H. J. Jodl, and Y. Crespo, Phys. Rep. **743**, 1 (2018).

[4] T. Nomura, Y. H. Matsuda, S. Takeyama, A. Matsuo, K. Kindo, J. L. Her, and T. C. Kobayashi, Phys. Rev. Lett. **112**, 247201 (2014).

[5] T. Nomura, Y. H. Matsuda, S. Takeyama, A. Matsuo, K. Kindo, and T. C. Kobayashi, Phys. Rev. B **92**, 064109 (2015).

[6] T. Nomura, Y. H. Matsuda, and T. C. Kobayashi, Phys. Rev. B **96**, 054439 (2017).

[7] S. Kasamatsu, T. Kato, and O. Sugino, Phys. Rev. B **95**, 235120 (2017).

[8] K. Katsumata, S. Kimura, U. Staub, Y. Narumi, Y. Tanaka, S. Shimomura, T. Nakamura, S. W. Lovesey, T. Ishikawa, and H. Kitamura, J. Phys.: Condens. Matter **17**, L235 (2005).

[9] K. Watanabe, Y. Watanabe, S. Awaji, M. Fujiwara, N. Kobayashi, and T. Hasebe, Adv. Cryog. Eng. Mater. **44**, 747 (1998).

[10] Y. H. Matsuda, Y. Ueda, H. Nojiri, T. Takahashi, T. Inami, K. Ohwada, Y. Murakami, and T. Arima, Phys. B (Amsterdam, Neth.) **346-347**, 519 (2004).

[11] Y. H. Matsuda, T. Inami, K. Ohwada, Y. Murata, H. Nojiri, Y. Murakami, H. Ohta, W. Zhang, and K. Yoshimura, J. Phys. Soc. Jpn. **75**, 024710 (2006).

[12] C. Broennimann, E. F. Eikenberry, B. Henrich, R. Horisberger, G. Huelsen, E. Pohl, B. Schmitt, C. Schulze-Briese, M. Suzuki, T. Tomizaki, H. Toyokawa, and A. Wagner, J. Synchrotron Radiat. **13**, 120 (2006).

[13] T. Inami, K. Ohwada, M. Tsubota, Y. Murata, Y. H. Matsuda, H. Nojiri, H. Ueda, and Y. Murakami, J. Phys.: Conf. Ser. **51**, 502 (2006).

[14] Z. Islam, J. P. C. Ruff, H. Nojiri, Y. H. Matsuda, K. A. Ross, B. D. Gaulin, Z. Qu, and J. C. Lang, Rev. Sci. Instrum. **80**, 113902 (2009).

[15] C. Uyeda, K. Sugiyama, and M. Date, J. Phys. Soc. Jpn. **54**, 1107 (1985).

[16] Y. Akahama, H. Kawamura, and O. Shimomura, Phys. Rev. B **64**, 054105 (2001).

[17] C. Uyeda, A. Yamagishi, and M. Date, J. Phys. Soc. Jpn. **57**, 3954 (1988).

[18] Here, the magnetization of liquid oxygen at 8 T is 24 emu/g [17] and the bulk modulus is estimated to be 1.12 GPa using the sound velocity (971 m/s) [24,25] and the density 1.187 g/cm^3 [24,26]. The $\Delta V/V$ is 2×10^{-4} at 8 T [17].

[19] A. Ikeda, T. Nomura, Y. H. Matsuda, S. Tani, Y. Kobayashi, H. Watanabe, and K. Sato, Rev. Sci. Instrum. **88**, 083906 (2017).

[20] A. Ikeda, Y. H. Matsuda, and H. Tsuda, Rev. Sci. Instrum. **89**, 096103 (2018).

[21] A. Ikeda, A. Shimizu, and Y. H. Matsuda (unpublished).

[22] S. Kimura and K. Kindo, *EPR in the 21st Century* (Elsevier, New York, 2002), p. 799.

[23] S. Kimura, K. Kindo, Y. Narumi, M. Hagiwara, H. Kikuchi, and Y. Ajiro, J. Phys. Soc. Jpn. **72**, 99 (2003).

[24] A. van Itterbeek and O. Verbeke, Cryogenics **1**, 77 (1960).

[25] T. Nomura, Y. H. Matsuda, S. Zherlitsyn, J. Wosnitza, and T. C. Kobayashi, arXiv:1906.01207.

[26] W. Pentermann and W. Wagner, J. Chem. Thermodyn. **10**, 1161 (1978).